

Carrier Recombination Times in Amorphous-Silicon Doping Superlattices

M. Hundhausen and L. Ley^(a)

Max-Planck Institut für Festkörperforschung, D-7000 Stuttgart 80, Federal Republic of Germany
and

R. Carius

Fachbereich Physik, Universität Marburg, D-3550 Marburg, Federal Republic of Germany
(Received 23 July 1984)

Doping superlattices, i.e., multilayer structures consisting of ultrathin ($50 \text{ \AA} \leq d \leq 400 \text{ \AA}$) n -type, intrinsic, and p -type layers of a -Si:H ($nipi$ structures), have been produced. Up to a tenfold increase in their infrared photoconductivity after band-gap illumination compared to unstructured a -Si:H is observed. The results are well described by a simple model for the carrier recombination kinetics that takes into account the spatial separation of electrons and holes due to the modulation of the band energies.

PACS numbers: 72.20.Jv, 68.55.+b, 71.25.Mg, 72.40.+w

The advances of molecular beam epitaxy have made possible the growth of complicated thin-layer semiconductor heterostructures that range from a few layers to compositional superlattices.¹ Another achievement of the same technique is the realization of doping superlattices, i.e., a system composed of a periodic sequence of ultrathin n - and p -doped semiconducting layers with, possibly, intrinsic layers of the same material in between.² Some of the unusual properties of these so-called " $nipi$ crystals" such as a tunable band gap and two-dimensional subbands have recently been reported for $nipi$ structures based on GaAs.³ It is but a small step to imagine superlattices based on amorphous hydrogenated silicon (a -Si:H), a material that is known to be dopable.⁴ Such a superlattice combines aspects of a crystalline periodic structure in the direction perpendicular to the layers with the amorphous nature of the material that it is based on.⁵

We have realized amorphous $nipi$ superlattices with layer thicknesses between 50 and 800 \AA and up to a total of 200 layers. The samples were prepared by the glow-discharge decomposition of SiH_4 in a computer-controlled continuous rf-plasma on quartz substrates held at a temperature of 350 $^\circ\text{C}$. Doping was achieved by adding alternately 100 ppm of PH_3 (n -type layer) or B_2H_6 (p -type layer) to SiH_4 . The individual layers were of equal thickness $d = d_i = d_n = d_p$ resulting in $nipi$ periods from 200 to 3200 \AA . The number of deposited layers was adjusted to give a total thickness of about 1 μm . The correct doping profile was confirmed by secondary-ion mass spectroscopy nuclear reaction techniques,⁶ and the selective etching of the n layer with CP6.

The regular alternation in the type of doping results in a periodic modulation of the band edge energies in a direction perpendicular to the film surface as depicted schematically in Fig. 1(a), whereas

the material is homogeneous and isotropic in the plane parallel to the surface. The modulation of the band energies is accompanied by built-in electric fields that are expected to act strongly on mobile charge carriers and thus affect their recombination kinetics. We have studied the recombination times of photoexcited carriers in $nipi$ structures using the transient infrared (ir) photoconductivity that is observed after the band-gap illumination has been turned off.⁷ The results of the measurements are explained in terms of a simple model which we shall describe first.

Referring to Fig. 1(a) we expect that a portion of the photoexcited electrons will drift to the conduction-band minima in the n layers while a portion of the holes accumulate near the valence-band maxima in the p layers. The recombination probability of these spatially separated carriers decreases

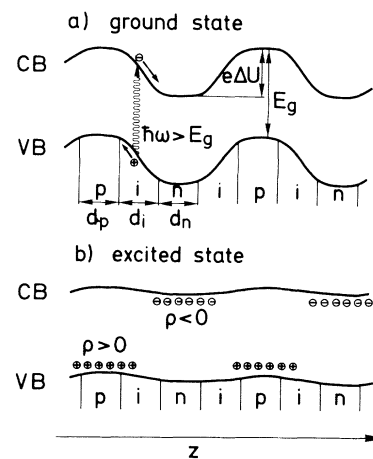


FIG. 1. Schematic real-space band diagram of a $nipi$ structure. (a) Equilibrium; (b) with a concentration of photoexcited carriers sufficient to reduce the band modulation.

drastically over that found in unmodulated specimens (see below and Ref. 2). As a result, electrons and holes will build up space charges which reduce the modulation amplitude ΔU of the band energies and thus also the magnitude of the electric fields [Fig. 1(b)]. The carrier density necessary to reduce ΔU to zero follows from Poisson's equation:

$$d^2U/dz^2 = (1/\epsilon_r\epsilon_0)\rho(z). \quad (1)$$

Assuming constant and equal but opposite charge densities $\rho_n = -\rho_p$ in the n and p layers, respectively, and $\rho = 0$ in the i layers the integration of Eq. (1) yields for the charge ρ_n necessary to offset a built-in modulation amplitude ΔU

$$\rho_n = -\Delta U \frac{4}{3} \epsilon_r \epsilon_0 / d^2, \quad (2)$$

where d is the thickness of the individual layers. Hence the maximum excess density of electron-hole pairs which can be trapped separated from each other is

$$N_{\max} = \frac{1}{4} \rho_n / e = \frac{1}{3} (\epsilon_r \epsilon_0 / e) d^{-2} \Delta U. \quad (3)$$

The factor $\frac{1}{4}$ takes into account that charges of either sign are only stored in one quarter of the $nipi$ repeat unit. With $\epsilon_r = 11$ and $\Delta U = 0.9$ eV, a value determined from differences in the activation energies of unstructured samples, we obtain $N_{\max} = 1.8 \times 10^{18} [(100 \text{ \AA})/d]^2 \text{ cm}^{-3}$. This number is, of course, only an estimate depending on the simplifying assumption of constant charge densities in the doped layers. If the density of carriers exceeds N_{\max} they are no longer separated by $nipi$ fields and behave like those in unmodulated $a\text{-Si:H}$ specimens.

At temperatures below ~ 30 K the recombination of trapped carriers proceeds via tunneling and their lifetime τ depends on the separation R between electron and hole or between carrier and recombination center according to

$$\tau(R) = \tau_0 \exp(2R/R_0). \quad (4)$$

In $a\text{-Si:H}$, $R_0 \sim 10 \text{ \AA}$ and the prefactor τ_0 is typically 10^{-12} sec for nonradiative and 10^{-8} sec for radiative tunneling, respectively.⁸

As a result of these considerations we expect the lifetime of the $nipi$ -field-separated carriers to increase with d according to Eq. (4) provided that d exceeds the average intrinsic separation R_{av} in unstructured samples. Likewise, their density is expected to vary like $1/d^2$ in accord with Eq. (3).

We use an excite-probe technique to test these predictions and the principle of operation of the experiment is shown in Fig. 2. Charge carriers are generated throughout the $nipi$ sample by band-gap light ($h\nu = 1.92$ eV) at temperatures below 30 K. When the light is turned off the carriers are trapped

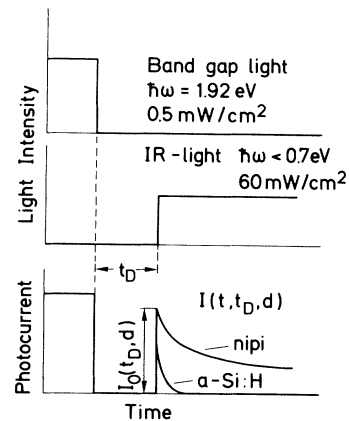


FIG. 2. Time diagram of the double-beam experiment employed to determine the density of trapped carriers (for details see text).

within 10^{-11} sec in tail states.⁷ Since no sizable thermal release of the trapped carriers occurs at the low temperature the nonequilibrium distribution starts to decay as dictated by the distribution of frozen-in distances according to Eq. (4). Illuminating the sample after a dark time t_D with sub-band-gap ir light ($h\nu \leq 0.7$ eV) excites the carriers above their respective mobility edges which results in a photocurrent transient $I(t, t_D, d)$. Intermeshed coplanar chromium electrodes with an effective gap of $0.4 \times 70 \text{ mm}^2$ were evaporated onto the samples which resulted in Ohmic contacts for applied voltages between 30 and 120 V, the range used here.

The initial amplitude of the current, $I_0(t_D, d) = I(0, t_D, d)$ is a measure of the nonequilibrium concentration of trapped band-tail carriers that survive the dark time t_D . Values of I_0 for $t_D = 1$ sec are plotted in Fig. 3 as a function of layer thickness d . The ir transient amplitude is governed by the $nipi$ effect for $50 \text{ \AA} \leq d \leq 300 \text{ \AA}$ and it is higher by up to an order of magnitude compared to a compensated⁹ (i.e., $d = 0$) or an undoped sample. We have convinced ourselves that the observed ir photoresponse is a bulk effect and not limited to the topmost layer by exciting carriers with strongly absorbed blue light ($h\nu = 2.4$ eV). We observe (a) a reduction in the amplitude of the photoresponse in accord with the reduced penetration depth of the light, and (b) the same effect independent of whether we illuminate from the front or the back.

The intensity of the exciting band-gap light exceeds that necessary to flatten the bands as shown in Fig. 1(b) and the photocurrent transient has therefore two contributions: one with a time constant long compared to t_D which is due to the separated carriers, and one due to randomly distri-

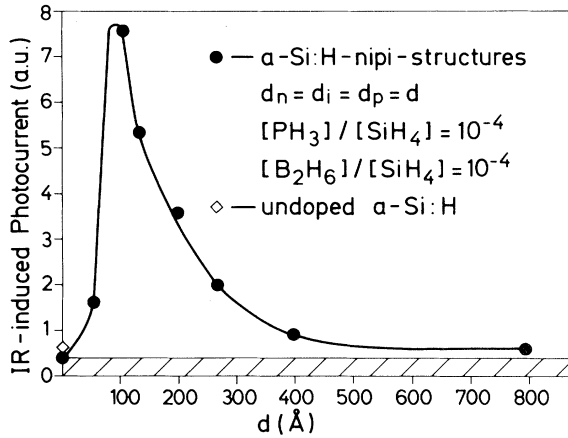


FIG. 3. Initial amplitude of the ir-induced photocurrent transient after a dark time of 1 sec plotted vs layer thickness d . The point for $d=0$ corresponds to a compensated sample. One unit in the photocurrent corresponds to 10^{-11} A for an applied voltage of 100 V.

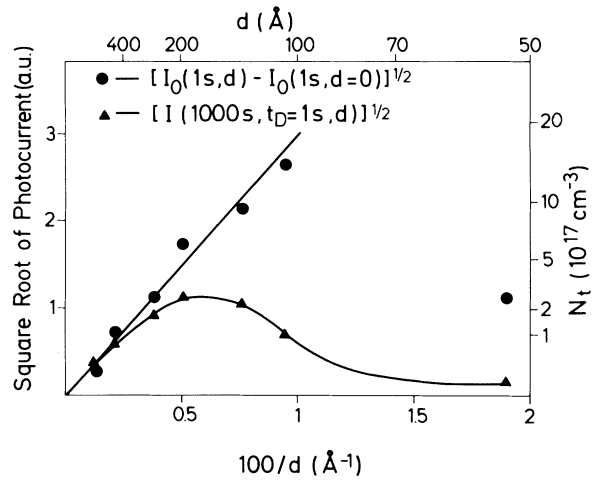


FIG. 4. Square root of the transient photocurrent vs $1/d$. Full circles correspond to the initial amplitude of the transient and triangles to its value 1000 sec later.

buted carriers which is much smaller on account of their short decay time [cf. Eq. (4)] and independent of d . We approximate the latter by the photocurrent of the compensated sample, $I_0(1 s, 0)$, and plot $[I_0(1 s, d) - I_0(1 s, d=0)]^{1/2}$ which is proportional to the saturation concentration of spatially separated carriers, $N_{max}^{1/2}$, vs $1/d$ in Fig. 4. The data points follow indeed a straight line through the origin and thus confirm nicely the first conclusion from our model as expressed in Eq. (3). For the $d = 50\text{-}\text{\AA}$ sample a dark time of 1 sec is too long to justify the interpretation of I_0 as a measure for the number of separated carriers [cf. Eq. (4)]. Also, the value of ΔU may be reduced from 0.9 eV for layers with a thickness of only 50 \AA . That is why the corresponding point does not conform to the linear relationship established by the other samples. Comparing the slope of the straight line in Fig. 4 with the numerical factor given in Eq. (3) we can calibrate our photocurrent amplitude in terms of N_t , the concentration of trapped carriers surviving the dark time t_D .¹⁰ The values for N_t so derived are given on the right-hand side of Fig. 4. For the compensated sample we obtain thus $N_t = 8 \times 10^{16} \text{ cm}^{-3}$ for $t_D = 1$ sec in agreement with values found for doped samples by light-induced ESR decay measurements.⁸

Detrapping of carriers by ir irradiation to levels above the mobility edge favors their recombination in unmodulated material due to retrapping near a carrier of opposite sign. As a result the "normal" ir-induced photocurrent disappears after sufficiently long irradiation times. This recombination path is

obstructed in *nipi* structures where the carriers remain separated by the electric fields which build up again as the sample returns to equilibrium. Thus the current transients remain high even after ir irradiation times as long as $t = 1000$ sec. $I(1000 \text{ s}, t_D = 1 \text{ s}, d)$ is also plotted in Fig. 4. For $d \geq 300 \text{ \AA}$ $I(1000 \text{ s}, t_D, d)$ is virtually unchanged compared to $I_{0, \text{nipi}}$, a fact that bears witness to the high stability of the nonequilibrium distribution in these samples.

An independent check of the increasing carrier lifetimes in *nipi* structures compared to unmodulated *a*-Si:H is to study the decay of the light-induced nonequilibrium distribution of trapped carriers with t_D directly by our double-beam experiment. In Fig. 5 the amplitude of the transient $I_0(t_D, d)$ is plotted as a function of t_D for various d . The curves are normalized to their values at $t_D = 1$ sec. The decay is obviously nonexponential, and so we define as the half-lifetime, $t_{D 1/2}$, the time when the signal drops to half of its initial value. This quantity is plotted versus d in the inset of Fig. 5. It is evident that $t_{D 1/2}$ increases exponentially with superlattice period for $d \geq 100 \text{ \AA}$ as expected from Eq. (4).

In summary, we have demonstrated the feasibility to produce *nipi* superlattices by the glow-discharge deposition of *a*-Si:H. The carrier recombination kinetics in these novel semiconducting elements deviates characteristically from that in unstructured material. The differences are well accounted for by a simple model that takes the modulation of the band energies into account. We expect to see further interesting developments in this new field of amorphous superlattices as a result of the

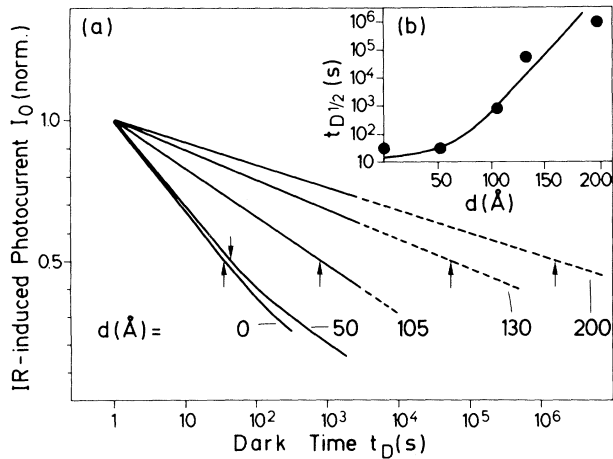


FIG. 5. (a) Amplitude of the ir-induced photocurrent as a function of the dark time after band-gap illumination t_D . Note the logarithmic time scale. The half-lifetimes $t_{D1/2}$ are marked with arrows. (b) $t_{D1/2}$ vs layer thickness d .

versatility in composition of amorphous semiconductors compared to their crystalline counterparts.

This work was initiated by the pioneering ideas of G. Döhler and we thank him for many stimulating discussions. We are indebted to W. Neu and F. Kübler for their expert technical support. We thank P. Eichinger for his help with the secondary-ion mass spectroscopy measurements and F. Ha-

braken for the nuclear reaction data.

(a) Present address: IBM T. J. Watson Research Center, Box 218, Yorktown Heights, N.Y. 10598.

¹See, e.g., L. Esaki, *J. Cryst. Growth* **52**, 227 (1981).

²G. H. Döhler, in *Advances in Solid State Physics: Festkoerperprobleme, Vol. 23*, edited by P. Grosse (Heyden, Philadelphia, 1983), p. 207.

³G. H. Döhler, H. Künzel, D. Olego, K. Ploog, P. Ruden, H. J. Stolz, and G. Abstreiter, *Phys. Rev. Lett.* **47**, 864 (1981).

⁴G. H. Döhler, *Verh. Dtsch. Phys. Ges.* **17**, 745 (1982).

⁵Compositional amorphous superlattices have been reported by a number of groups: B. Abeles and T. Tiedje, *Phys. Rev. Lett.* **51**, 2003 (1983); H. Munekata and H. Kukimoto, *Jpn. J. Appl. Phys.* **22**, L544 (1983); J. Kakalios, H. Fritzsche, N. Ibaraki, and S. R. Ovshinsky, *J. Non-Cryst. Solids* **66**, 339 (1984); M. Hirose and S. Miyazaki, *J. Non-Cryst. Solids* **66**, 327 (1984).

⁶W. A. Lanford, H. P. Trautwetter, J. F. Ziegler, and J. Keller, *Appl. Phys. Lett.* **28**, 566 (1976).

⁷M. Hoheisel, R. Carius, and W. Fuhs, *J. Non-Cryst. Solids* **59&60**, 457 (1983).

⁸D. K. Biegelsen, R. A. Street, and W. B. Jackson, *Physica (Utrecht)* **117&118B**, 899 (1983).

⁹The compensated sample was prepared with 25 ppm PH_3 and 25 ppm B_2H_6 . This results in the same average impurity concentration as that in the *nipi* structures.

¹⁰In doing so we tacitly assume that $I_0(1, d) \sim I_0(0, d)$ for the *nipi* structures with $d > 50 \text{ \AA}$.